

ARTICLES

Shape-Controlled Synthesis of Palladium Nanorods and Their Magnetic Properties

Congwen Xiao, Hao Ding, Chengmin Shen, Tianzhong Yang, Chao Hui, and H.-J. Gao*

*Beijing National Laboratory for Condensed Matter Physics, Institute of Physics, Chinese Academy of Sciences, Beijing, 100190, China**Received: March 4, 2009; Revised Manuscript Received: June 19, 2009*

A simple method for the controlled growth of single crystalline palladium nanorods is presented. Through tuning the molar ratio of two surfactants, cetyltrimethylammonium bromide (CTAB) and poly(vinyl pyrrolidone) (PVP), single crystalline palladium nanorods with different aspect ratios can be synthesized in large quantities. The introduction of cosurfactant CTAB is critical to the growth of palladium nanorods. Its headgroup CTA⁺ and counterion Br⁻ anion act as stabilizing species and etchant, respectively. Compared with PVP-capped Pd nanoparticles, the Pd nanorods show a ferromagnetism behavior at 5 and 300 K, respectively.

Introduction

Palladium plays an important catalytic role in many foundational research and practical applications. For instance, cross-coupling reactions of aryl halides with arylboronic acids (Suzuki coupling reactions) and the coupling of aryl halides with alkenes (Heck reaction) are important organic reactions catalyzed by palladium.¹ It also serves as a major catalyst in automobile industry for the reduction of vehicle exhausts.² Moreover, Pd shows a very large capacity for hydrogen absorption, and its structural change involved in the adsorption process offers a number of attractive features suitable for energy purposes.³ Recent reports show that nanoscale palladium and general 4d transition metals nanoparticles have novel magnetic properties. Though a free Pd atom has a [Kr] 4d¹⁰ configuration and it is nonmagnetic according to the Hund rule, the configuration changes when a group of Pd atoms form a crystalline structure, with a few electrons shifting from 4d to 5s. With a configuration of 4d^(10-a)5s^a ($a \geq 0$), bulk Pd exhibits enhanced Pauli paramagnetism with large susceptibility. Although no spontaneous ferromagnetic order exists in bulk Pd, it lies the closest to fulfilling the Stoner criterion of 4d transitional metals, $N(E)I > 1$, where $N(E)$ and I stand for the density of states just below the Fermi level (E_f) and the Stoner parameter, respectively (typically 1.23 state/eV spin atom and 0.71 eV for Pd). In confined nanoscale systems, more localized electronic states as well as narrower bands are usually supposed to increase the densities of states and lead to the exotic magnetic behavior.⁴ The ferromagnetic behavior of Pd was first experimentally recorded in 1997, when the Taniyama group observed the appearance of a magnetic moment in pure Pd clusters synthesized by gas evaporation.⁵

In a subsequent study, they reported the susceptibility increases with a decrease in Pd cluster size from 9.9 to 5.9 nm by the same CVD method.⁶ Later, Sampedro et al. observed ferromagnetism in 2.4 nm twinned Pd NPs capped by surfactants.⁷ More recently, Teng et al. successfully obtained Pd polycrystalline nanowires via a modified phase-transfer method.

This unique quasi-1D system also shows distinctive ferromagnetic behavior from Pd nanoparticles.⁸ Although diversified in preparation methods and restricted to 0D or quasi-1D nanomaterials, these studies demonstrated well the feasibility of tuning the magnetic property of Pd at the nanoscale, which will facilitate both the understanding of fundamental magnetism and the future application of spintronic technology.⁹

Attempting to take full advantage of those properties, people developed various methods to synthesize palladium nanostructures with desired morphologies. Palladium nanoparticles with different shapes, such as cube,¹⁰ bar,¹¹ cuboctahedron,¹² hexagon,¹³ triangle,¹⁴ and hollow sphere,¹⁵ have been successfully synthesized by electrodeposition,¹⁶ thermal decomposition of palladium complexes,¹⁷ reduction of palladium salts in specific templates,^{12,14,18} selective etching,^{14,19} or via a coordinating ligand.²⁰ Compared to the wide variety of zero-dimensional nanostructures, synthesis of one-dimensional (1D) palladium nanostructures is mainly limited to mesoscale, polycrystalline wires or tubes.²¹ Despite all these efforts, it remains a great challenge to achieve shape-controlled synthesis of single crystalline palladium nanostructures in a large scale, particularly the 1D structure. The solution phase method is widely applied in the synthesis for nanostructures of transition metal elements.^{22–24} In this article, we report a synthetic approach toward single-crystalline Pd nanorods with a controlled aspect ratio in large quantities via a simple one-pot solution method. The ferromagnetic properties of Pd nanorods were observed at room temperature, and the onset of ferromagnetic behavior was proved to be highly related to the unique 1D growth behavior.

Experimental section

Materials. Ethylene glycol (EG), poly(vinyl pyrrolidone) (PVP, MW = 58 000), and cetyltrimethylammonium bromide (CTAB), were purchased from Acros Company; H₂PdCl₄ and NaBr were purchased from Beijing Chemistry Reagent Lt. All reagents were used without further purification.

Synthesis of Palladium Nanorods. In our approach, palladium salts were reduced by the popular polyol method.²⁵ EG was used as both solvent and reductant, whereas PVP acted as

* Corresponding author. E-mail: hjgao@aphy.iphy.ac.cn.

surfactant. The growth of palladium rods could be achieved by introducing a cosurfactant, CTAB. In a typical synthesis, a solution of 0.6 mmol PVP was mixed with 10 mL of EG in a three-neck flask and heated at 150 °C for 1 h under argon flow. Ten minutes after the injection of 2 mL aqueous CTAB solution (0.09 M) into the flask, 1 mL of aqueous H_2PdCl_4 (0.125 M) solution was added in the solution with vigorous stirring. The solution was then kept at 150 °C for 30 min and cooled to room temperature. The product was precipitated by acetone and washed with ethanol four times to remove excess EG and surfactants. The final black product could be easily redispersed in polar solvents such as ethanol and water to yield a clear homogeneous solution.

Characterization of Pd Nanorods. The morphology of the samples was investigated by transmission electron microscopy (TEM), high resolution transmission electron microscopy (HR-TEM), and selected area electron diffraction (SAED). TEM samples were prepared by placing one drop of the solution on a carbon-coated copper grid. The X-ray diffraction (XRD) pattern of the product was recorded on a Rigaku D/MAX 2400 X-ray diffractometer with Cu $K\alpha$ radiation source ($\lambda = 1.5405 \text{ \AA}$). Electron energy loss spectroscopy (EELS) was used to identify the chemical compositions of the Pd nanorods. Magnetic measurement was performed in MPMS-5 superconducting quantum interference device (SQUID) magnetometry.

Results and discussion

The anisotropic crystal structure or crystal surface reactivity, for instance, $\{110\} > \{111\} > \{100\}$ in face-centered cubic (fcc) structure, was identified in the literature as the two main mechanisms for the growth of one-dimensional nanostructure. With highly symmetric fcc structure, anisotropic growth of palladium can be achieved only by the latter one, similar to the growth of Ag and Au nanorods.²⁶ As a long chain polymer with a carbonyl group, PVP can adsorb on metal nanoparticles and protect them from aggregation. Polygonal palladium nanoparticles are often obtained when using PVP as a surfactant due to its selective adsorption on $\{111\}$ and $\{100\}$ facets.^{14,19} However, one-dimensional growth is rarely observed in these cases. In our approach, the addition of CTAB is critical to induce the growth of nanorods. Though CTAB cannot provide enough capping ability alone in the polyol method and we found only aggregated particles can be obtained without the assistance of PVP, it cooperates well with PVP molecules in the shape control of palladium nanostructure. Through tuning the CTAB/PVP ratio, palladium rods with different aspect ratios were readily prepared.

Figure 1A and B shows typical TEM images of palladium nanorods with average aspect ratios of 7.8 (length, $18.3 \pm 1.6 \text{ nm}$; width, $2.5 \pm 0.3 \text{ nm}$) and 2.5 (length, $6.5 \pm 0.7 \text{ nm}$; width, $2.7 \pm 0.3 \text{ nm}$), respectively. These nanorods tend to assemble into a 1D ribbon-like structure with parallel lateral edges. Such side-by-side alignment can be ascribed to the interactions among the organic stabilizing ligands surrounding the nanorods. It should also be noted that only nanorods with a relatively narrower distribution of aspect ratio can self-assemble into such regular structures. Figure 1C shows the HRTEM image of a typical Pd nanorod with well-defined lattice planes. From the further magnified image in the inset of 1C, the lattice spacing is 1.95 and 2.26 Å, corresponding to the lattice spacing of $\{200\}$ and $\{111\}$, respectively, for fcc palladium. The fast Fourier transform analysis in the inset confirms their $\langle 100 \rangle$ growth direction. The appearance of a high-energy $\{110\}$ side surface suggests thermodynamic growth induced by the surfactant.²⁷ For

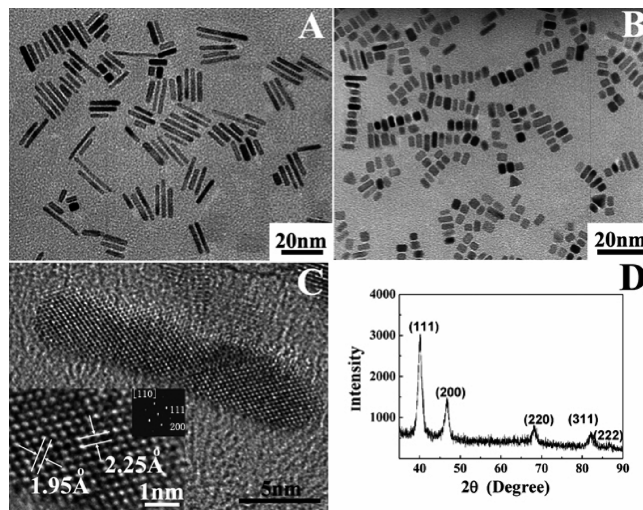


Figure 1. TEM images of palladium nanorods with different aspect ratios synthesized by varying the $n_{\text{CTAB/PVP}}$. (A) $n_{\text{CTAB/PVP}} = 0.3$ and (B) $n_{\text{CTAB/PVP}} = 0.8$. (C) HRTEM image of several nanorods with well-defined lattice planes, confirming the single crystalline structure of these nanorods. Atomic resolution image of one end of an individual nanorod is shown in the lower left-hand corner of panel C. The fast Fourier transform shows the $[100]$ growth direction (in the upper right-hand corner of the inset). (D) XRD pattern of Pd nanorods with an aspect ratio of 7.8.

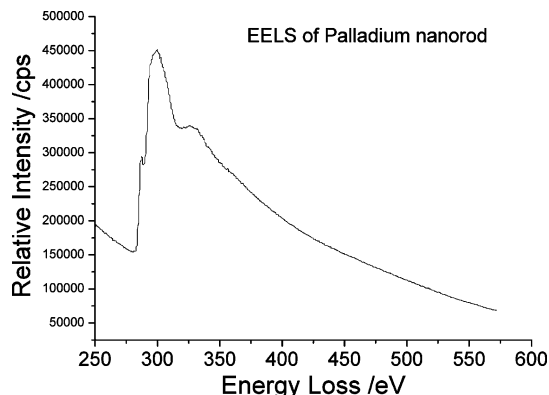


Figure 2. Electron energy loss spectroscopy of several Pd nanorods. The Pd M-shell and C K-shell ionization edges were observed around 335 and 285 eV, respectively. No oxygen K-shell peak was detected, indicating these Pd nanorods are pure Pd and no surface oxidation occurs.

palladium nanoparticles reported with a regular shape, such as a cube, cuboctahedron, or prism, their surfaces are usually bound by low-energy $\{100\}$ and $\{111\}$ facets. The high-energy $\{110\}$ facet is rarely observed in palladium nanostructures. The ends of palladium nanorods are terminated by $\{001\}$ and $\{111\}$ facets of small areas. A similar structure was observed in 1D gold nanostructures synthesized by using CTAB as the surfactant.²⁷

The crystal structure of the Pd nanorods was characterized by XRD. Figure 1D shows the XRD pattern of Pd nanorods with an aspect ratio of 7.8. The reflection peaks can be indexed to a fcc crystalline structure of Pd (JCPDS, Card No.46-1043). Further EELS analysis (Figure 2) of these nanorods reveals they are composed of pure metallic Pd and no surface oxidation occurs.

Using a combination of two surfactants for the fine control of nanoparticle growth is well-adopted in nonaqueous synthesis of anisotropic semiconductor and magnetic nanomaterials. For instance, two molecules with different coordinating ability, hexyl phosphonic acid and trioctylphosphine oxide, were adopted in

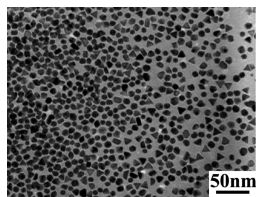


Figure 3. TEM image of polyhedral Pd nanoparticles prepared using PVP alone as the surfactant.

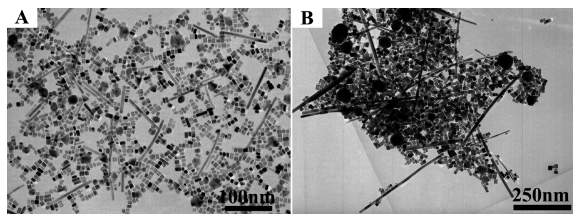


Figure 4. TEM images of the product synthesized at high molar ratio of CTAB and PVP. (A) $n_{\text{CTAB/PVP}} = 2$ and (B) $n_{\text{CTAB/PVP}} = 4$. The final products consist of a mixture of nonuniform nanorods and irregular particles.

the synthesis of CdSe nanorods.²⁸ However, it is somewhat different in our case. We believe CTAB plays a multiple role in the formation of Pd nanorods. First, the CTA⁺ headgroup of CTAB has been proved to form a bilayer structure on the surface of metal nanoparticles and stabilize them.²⁶ With weaker coordinating ability compared with PVP at high temperature, CTAB acts as a cosurfactant to direct the anisotropic growth. Another factor is Br⁻ anions from CTAB surfactant molecules. The existence of specific anions has been proven to be an effective route for the controlled synthesis of metal nanostructures.^{29,30} In our experiment, it was found that an increase in CTAB concentration would have an effect on the morphology of the palladium nanostructure. Without CTAB, only polyhedral Pd nanoparticles can be obtained (Figure 3). Uniform nanorods with different aspect ratios can be achieved at a molar ratio of CTAB to PVP ranging from 0.3 to 0.8, as seen from Figure 1. When the molar ratio changes to between 2.0 and 4.0, mixtures of nonuniform Pd nanorods and irregularly shaped nanoparticles were observed. The results are shown in Figure 4. It is not surprising, since the enhanced ion etching of Br⁻ with increased CTAB concentration will lower the deposition velocity of Pd atoms on all crystal facets indiscriminately. This effect reduces the difference of growth speed for various crystal facets and, thus, leads to less anisotropic shapes, usually irregularly faceted nanoparticles.

Magnetic properties of Pd nanorods at different temperatures were measured by SQUID. To eliminate the influence of size deviation as much as possible, the sample with an aspect ratio of 2.5 was chosen for the measurement. Room temperature ferromagnetic behavior of Pd nanorods can be clearly observed from the hysteresis loops shown in Figure 5. The coercive field (H_c) of Pd nanorods decreases with increasing measurement temperature: 112 Oe at 5 K, 80 Oe at 150 K, and 69 Oe at 300 K. In addition, it is observed that the magnetization is not saturated at any temperature. This may be due to the existence of superparamagnetic and paramagnetic atoms in the particles. It may be argued that the observed behavior is due to the presence of surplus surfactants or surface oxidation. However, the M–H curve of PVP shown in Figure 5B indicates that the polymer surfactant is diamagnetic. Combined with the EELS analysis, which excluded the existence of oxygen, it can be concluded that a permanent magnetic moment is an intrinsic property of a Pd nanorod.

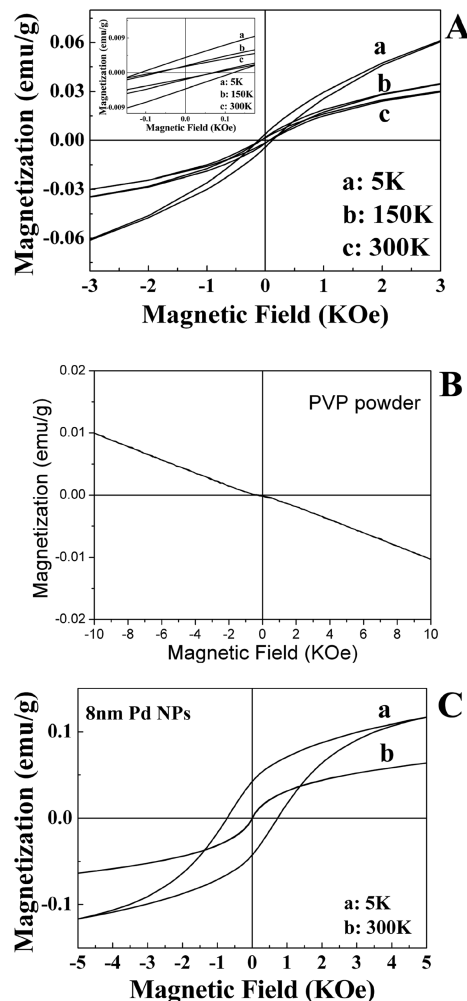


Figure 5. M–H curves of Pd nanorods and spherical nanoparticles at different temperatures. (A) M–H curves of Pd nanorods at 5, 150, and 300 K; (B) M–H curve of PVP at room temperature, indicating the diamagnetic nature of the surfactant; and (C) M–H curves of 8 nm spherical Pd nanoparticles at 5 and 300 K.

Figure 5C shows the hysteresis loop curve of 8 nm spherical PVP-capped Pd nanoparticles synthesized by a similar polyol process. The spherical Pd nanoparticles are ferromagnetic at low temperature (5 K) and superparamagnetic at room temperature. Compared with these results, Pd nanorods show different magnetic behavior at room temperature. This interesting phenomenon clearly indicates the peculiar morphology of Pd nanorods leads to a magnetic behavior distinct from its 0D counterpart in the same synthetic system. The crystal shape is an important factor here, since the less demagnetizing field along growth direction $\langle 100 \rangle$ will make it an easier axis of magnetization, whereas spherical particles have no such shape anisotropy. High shape anisotropy energy has already been proven to be able to significantly enhance the blocking temperature of magnetic materials such as Co, Fe, and FePt. Moreover, we suggest the unique surface structure of Pd nanorods also plays a key role in this phenomenon. The reduced degree of coordination of surface atoms and the interaction between those and the capping molecules, both of which are determined by surface structure, are well-recognized to lead to more localized electronic states and the onset of ferromagnetism for 4d and 5d noble metals. In our experiment, the surfaces of the Pd nanoparticle are composed of only low-energy $\{100\}$ and $\{111\}$ facets, whereas Pd nanorods have a much higher ratio of $\{110\}$ facets at their side surfaces. The different nature between crystal

facets might account for the distinctive magnetism. Previous theoretical calculation from Felix Yndurain et al. also predicted that various crystal facets of fcc Pd would have different magnetic behavior and a change in the magnetic moment might even come from the same facet along different orientations.³¹ Although the detailed mechanism is still elusive, the morphology-related magnetism is believed to be meaningful in the exploration of novel magnetism in other nonmagnetic metals at nanoscale, such as Au and Ag.^{32,33}

In summary, we have developed a simple synthetic method for single crystalline Pd nanorods with controlled morphology. The anisotropic growth of Pd nanorods derived from introducing CTAB as a cosurfactant. The palladium nanorods have a narrow size distribution and uniform shape, and their aspect ratio can be tuned through controlling the molar ratio of CTAB to PVP molecules. These Pd nanorods show unique ferromagnetic behaviors at room and lower temperature. They may have potential applications in various fields, such as high-density information storage and spintronic devices.

Acknowledgment. This project is supported in part by the National Science Foundation of China (Grant No. 50872147), and the National “973” project of China.

References and Notes

- (1) Narayanan, R.; El-Sayed, M. A. *Langmuir* **2005**, *21*, 2027.
- (2) Nishihata, Y.; Mizuki, J.; Kao, T.; Tanaka, H.; Enishi, M.; Imura, M.; Kamoto, T.; Hamada, N. *Nature* **2002**, *418*, 164.
- (3) Favier, F.; Walter, E. C.; Zach, M. P.; Benter, T.; Penner, R. M. *Science* **2001**, *293*, 2227.
- (4) Liu, X.; Bauer, M.; Bertagnolli, H.; Roduner, E.; Slageren, J.; Philipp, F. *Phys. Rev. Lett.* **2006**, *97*, 253401.
- (5) Taniyama, T.; Ohta, E.; Sato, T. *Europhys. Lett.* **1997**, *38*, 195.
- (6) Shinohara, T.; Sato, T.; Taniyama, T. *Phys. Rev. Lett.* **2003**, *91*, 197201.
- (7) Sampedro, B.; Crespo, P.; Hernando, A.; Litran, R.; Sanchez Lopez, C.; Lopez Cartes, C.; Fernandez, A.; Ramirez, J.; Gonzalez Calbet, J.; Vallet, M. *Phys. Rev. Lett.* **2003**, *91*, 237201.
- (8) Teng, X. W.; Han, W. Q.; Ku, W.; Hucker, M. *Angew. Chem., Int. Ed.* **2008**, *47*, 2055.
- (9) Hernando, A.; Crespo, P.; García, M. A.; Fernández Pinel, E.; de la Venta, J.; Fernández, A.; Penadés, S. *Phys. Rev. B* **2006**, *74*, 052404.
- (10) Xiong, Y. J.; Chen, J. Y.; Wiley, B.; Xia, Y. A.; Yin, Y. D.; Li, Z. Y. *Nano Lett.* **2005**, *5*, 1237.
- (11) Xiong, Y. J.; Cai, H. G.; Wiley, J. B.; Wang, J. G.; Kim, M. J.; Xia, Y. N. *J. Am. Chem. Soc.* **2007**, *129*, 3665.
- (12) Veisz, B.; Kiraly, Z. *Langmuir* **2003**, *19*, 4817.
- (13) Gugliotti, L. A.; Feldheim, D. L.; Eaton, B. E. *Science* **2004**, *304*, 850.
- (14) Xiong, Y. J.; McLellan, J. M.; Chen, J. Y.; Yin, Y. D.; Li, Z. Y.; Xia, Y. N. *J. Am. Chem. Soc.* **2005**, *127*, 17118.
- (15) Kim, S. W.; Kim, M.; Lee, W. Y.; Hyeon, T. *J. Am. Chem. Soc.* **2002**, *124*, 7642.
- (16) Yun, M. H.; Myung, N. V.; Vasquez, R. P.; Lee, C. S.; Menke, E.; Penner, R. M. *Nano Lett.* **2004**, *4*, 419.
- (17) Son, S. U.; Jang, Y.; Yoon, K. Y.; Kang, E.; Hyeon, T. *Nano Lett.* **2004**, *4*, 1147.
- (18) Ding, J. H.; Gin, D. L. *Chem. Mater.* **2000**, *12*, 22.
- (19) Xiong, Y. J.; Wiley, B.; Chen, J. Y.; Li, Z. Y.; Yin, Y. D.; Xia, Y. N. *Angew. Chem., Int. Ed.* **2005**, *44*, 7913.
- (20) Teranishi, T.; Miyake, M. *Chem. Mater.* **1998**, *10*, 594.
- (21) Yu, S. F.; Welp, U.; Hua, L. Z.; Rydh, A.; Kwok, W. K.; Wang, H. H. *Chem. Mater.* **2005**, *17*, 3445.
- (22) Hui, C.; Shen, C. M.; Yang, T. Z. *J. Phys. Chem. C* **2008**, *112*, 11336.
- (23) Yang, H. T.; Shen, C. M.; Su, Y. K.; Yang, T. Z.; Gao, H. J.; Wang, Y. G. *Appl. Phys. Lett.* **2003**, *82*, 4729.
- (24) Shen, C. M.; Su, Y. K.; Yang, H. T.; Yang, T. Z.; Gao, H. J. *Chem. Phys. Lett.* **2003**, *373*, 39.
- (25) Sun, Y. G.; Xia, Y. N. *Science* **2002**, *298*, 2176.
- (26) Murphy, C. J.; San, T. K.; Gole, A. M.; Orendorff, C. J.; Gao, J. X.; Gou, L.; Hunyadi, S. E.; Li, T. *J. Phys. Chem. B* **2005**, *109*, 13857.
- (27) Wang, Z. L. *J. Phys. Chem. B* **2000**, *104*, 1153.
- (28) Manna, L.; Scher, E. C.; Alivisatos, A. P. *J. Am. Chem. Soc.* **2000**, *122*, 12700.
- (29) Filankembo, A.; Giorgio, S.; Lisiecki, I.; Pileni, M. P. *J. Phys. Chem. B* **2003**, *107*, 7492.
- (30) Wiley, B. J.; Xiong, Y. J.; Li, Z. Y.; Yin, Y. D.; Xia, Y. N. A. *Nano Lett.* **2006**, *6*, 765.
- (31) Alexandre, S. S.; Anglada, E.; Soler, J. M.; Yndurain, F. *Phys. Rev. B* **2006**, *74*, 054405.
- (32) Suber, L.; Fiorani, D.; Scavia, G.; Imperatori, P.; Plunkett, W. R. *Chem. Mater.* **2007**, *19*, 1509.
- (33) Crespo, P.; Litran, R.; Rojas, T. C.; Multigner, M.; de la Fuente, J. M.; Sanchez-Lopez, J. C.; Garcia, M. A.; Hernando, A.; Penades, S.; Fernandez, A. *Phys. Rev. Lett.* **2004**, *93*, 087204.

JP902005J